Computing Discrete Minimal Surfaces and Their Conjugates

Ulrich Pinkall
Techn. Univ. Berlin
Sonderforschungsbereich 288
Strasse des 17. Juni
1000 Berlin 12
Germany

Konrad Polthier
Math. Inst. Univ. Bonn
Sonderforschungsbereich 256
Beringstr. 4
5300 Bonn 1
Germany

February 1993

Abstract. We present a new algorithm to compute stable discrete minimal surfaces bounded by a number of fixed or free boundary curves in $\mathbf{R}^3$, $\mathbf{S}^3$ and $\mathbf{H}^3$. The algorithm makes no restriction on the genus and can handle singular triangulations. For a discrete harmonic map a conjugation process is presented leading in case of minimal surfaces additionally to instable solutions of the free boundary value problem for minimal surfaces. Symmetry properties of boundary curves are respected during conjugation.

1. Introduction

The Problem of Plateau was a long standing problem in minimal surface theory. It asks for the existence of a disk type minimal surface spanned by a given closed boundary curve Γ in $\mathbf{R}^n$. The name honors the work of the Belgian physicist J.A. Plateau, who did extensive experimental studies during the beginning of the 19th century convincing the mathematicians of an affirmative solution of the question. But time had to pass until 1930 to create a theoretical proof: the use of the Weierstraß representation formulas had failed as well as trying to minimize the area functional

$$A(f) = \int_\Omega Jacobian(f)$$

in the class of parametric maps from a fixed disk-type domain $\Omega \subset \mathbf{R}^2$

$$\begin{aligned} f &: \Omega \to \mathbf{R}^n \\ f(\partial\Omega) &= \Gamma. \end{aligned}$$

Douglas [4] and Rado [11] at the same time had the ingenious idea not to minimize the area functional directly but to minimize, in the later reformulation by Courant [3], the Dirichlet integral

$$E_D(f) = \frac{1}{2}\int_\Omega |\nabla f|^2 .$$

By this the symmetries of the problem were drastically reduced from the class of all parameterizations to the class of all conformal parameterizations.

From the numerical point of view there exist a number of different methods to compute minimal surfaces, see for example [1], [2], [5], [13], [15], [16]. In this paper we present a new algorithm by splitting the minimization process in a sequence of steps computing harmonic maps on surfaces. We avoid using any two dimensional parameter domain. We will also minimize w.r.t. variations of boundary points lying on straight boundary lines, and points lying on free boundary curves restricted to planes. Therefore the resulting discrete minimal surfaces may be extended along boundary symmetry lines as discrete minimal surfaces.

Additionally we present for discrete harmonic maps an algorithm computing a conjugate harmonic map. In case of a planar surface this leads exactly to the conjugate minimal surface. If the image of a harmonic map has symmetry lines, then the conjugate image will have the corresponding symmetry properties, see §2 Since for minimal surfaces the identity map is harmonic we can compute its conjugate minimal surface using the above algorithm.

In the following we mention two major approaches for computing minimal surfaces in more detail since our algorithm is in some sense a mixture of both.

The first algorithm has its origin in the theoretical existence proofs of Douglas and Rado, resp. the later formulation by Courant, and tries to imitate them numerically: for a given curve $\Gamma \subset \mathbf{R}^3$ this algorithm works on discrete surfaces parameterized over the triangulated unit disk B. Starting with an initial parameterization

$$\begin{aligned} f : B \to \mathbf{R}^3 \\ f(\partial B) = \Gamma \end{aligned}$$

one successively repeats a two component minimization step:

- minimize the Dirichlet energy $E_D(f)$ by varying points in image space
- minimize $E_D(f)$ by varying points of the discretization in the planar domain B.

In the following we will call the first step the "Dirichlet step" and the second step the "conformal step", since it is used to make the map f conformal, see §2 for more details. During the Dirichlet step a fixed parameter domain is assumed. The numerical minimization of the Dirichlet integral is then a linear problem and straight forward. But for the conformal step the different algorithms vary, see e.g. Wohlrab [16] and Hutchinson [6].

Varying points in the domain may be interpreted as variation of the metric to make the map conformal. In the continuous case this would be accomplished by taking the induced metric, and the map would be immediately an isometry and therefore conformal. In the discrete case we even have the problem to define conformality. For example it is usually not possible to get a conformal map in the sense that angles in corresponding domain and image triangles are the same, since the domain is flat. It remains that one can minimize the conformal energy but without hope of getting it vanished.

Another approach to compute minimal surfaces is via mean curvature flow. Numerically this is the most natural approach since the area is directly minimized by letting the surface flow in normal direction with speed being the mean curvature of the surface. This equals minimizing in direction of the area gradient. One difference of this approach to the former one is that it only works in image space without having a two dimensional parameter domain. Implementations of such algorithms are due to Brakke [1] and Dziuk [5]. A drawback of this approach is that boundary points may vary only orthogonal to the curve, and that singularities develop in general at thin necks, even if the boundary curve is planar.

Our minimization algorithm combines aspects of both methods: it uses as the fundamental minimization step the Dirichlet step from the first algorithm but in a different way: for a given boundary Γ and metrical surface M_i we compute the next surface M_{i+1} as the minimizer of the Dirichlet functional

$$M_{i+1} := \min_{M} \frac{1}{2} \int_{M_i} |\nabla(f : M_i \to M)|^2 .$$

Pay attention to the fact that we do not use a planar two-dimensional domain but instead the most recent computed surface M_i. Such a trick was also applied in computing the mean curvature flow by Dziuk [5] to reduce numerical difficulties with the Laplace operator.

Numerically we are left within each step with a linear problem of computing the surface M_{i+1} where the minimum of the quadratic function is attained. This new minimization method is faster than the first algorithm since the nonlinear conformal step is completely skipped. It is no longer necessary to adapt the conformal structure of the parameter domain because in each step we start with the conformal identity map. This avoids also numerical inaccuracies arising from inaccurate conformal structures in the domain.

Since we always step to the absolute minimum of the Dirichlet integral in each iteration and do not move along the area gradient we proceed discrete also in time direction. Compared to the mean curvature flow we have therefore less problems with mean curvature type singularities arising e.g. at thin handles, see fig. 12, and we have more flexibility in moving points tangential to the boundary.

Additional to both theoretical algorithms we can handle in a natural way situations where lines are joined by multiple surfaces, see fig. **??**. Brakke's evolver can handle these too.

For the numerical and graphical computations the authors used the mathematical programming environment GRAPE developed at the Sonderforschungsbereich 256 at the University of Bonn.

This work was done while the second author visited the Sonderforschungsbereich 288 in Berlin. He wants to thank the SFB for the hospitality he enjoyed.

The authors would like to thank U. Brehm for fruitful discussions.

2. General Setup

Before we start with the discrete situation let us review a few definitions and results from the continuous case.

Let $\Gamma = \{\Gamma_1,..,\Gamma_n\}$ be a collection of Jordan curves and M a surface with boundary $\partial M = \Gamma$.

Definition 1. *M is a* **minimal surface** *iff for each point $p \in M$ one can choose a small neighbourhood $U(p)$ which has minimal area among other patches V having the same boundary as U.*

By this definition minimal surfaces are characterized by having locally least area compared to small variations of the surface.

Let (N, h) and(M, g) be two Riemannian manifolds with metrics h and g, and let

$$f : \Omega \subset N \to M$$

be a parameterization of a surface $f(\Omega) \subset M$ over a two dimensional domain submanifold $\Omega \subset N$. Then the *area* of $f(\Omega)$ is given by

$$\mathrm{A}(f) = \int_\Omega Jacobian(f)$$

and the *Dirichlet energy* of the map f is defined as

$$E_D(f) = \frac{1}{2} \int_\Omega |\nabla f|_g^2,$$

where $|\nabla f|_g^2 = trace\ g(\partial f., \partial f.)$, g indicating the metric to be used.

It is well known that

$$A(f(M)) \leq E_D(f)$$

with equality iff f is a conformal map. Following a proposal of Hutchinson [6] we will call the difference

$$E_C(f) = E_D(f)\text{-}A(f(M))$$

the *conformal energy* of the map f . This is justified by the observation that for Euclidean (x, y)-domains

$$E_C(f) = \frac{1}{2}\int_\Omega \left|D^{90} f_x - f_y\right|^2,$$

where D^{90} is the $90°$ rotation in the oriented tangent plane, is a natural measure of failure for a map to be conformal.

Minimal surfaces in three dimensional space forms $M^3(c)$ with constant curvature c always come in a family of minimal surfaces. Let $f : \Omega \to M^2 \subset M^3(c)$ be a minimal immersion of a simply connected domain Ω into a three dimensional space form. Then there exists the *associated family*

$$f^\theta : \Omega \to M^3(c)$$

of isometric minimal immersions: let g be the by f induced metric on Ω and S the Weingarten map defined by $\nabla f \cdot S = \nabla N$ with N being the normal map of the surface. Using these data the maps f^θ are determined up to isometrics of $M^3(c)$ by the geometric data (g^θ, S^θ) defined by

$$\begin{aligned} g^\theta &:= g \\ S^\theta &:= D^\theta \cdot S \ , \end{aligned} \tag{1}$$

where D^θ is rotation about the angle θ in the oriented tangent planes of Ω . $f^{\frac{\pi}{2}}$ is called the *conjugate immersion* of f, and $f^\pi = \mathit{inversion}(f)$. See Lawson[9] for a more detailed explanation.

Minimal surfaces in three dimensional space forms have a useful symmetry property: if they contain a straight line, i.e. a geodesic of $M^3(c)$, then the minimal surface is invariant under $180°$ rotation around this line, and if they meet a totally geodesic plane in $M^3(c)$ orthogonally along an arc, then the minimal surface is invariant under reflection at this plane. These properties allow the construction of complete surfaces from fundamental pieces bounded by symmetry lines.

The symmetry properties are also an essential tool for the existence proof called *conjugate surface construction*: This construction, originally invented by Smyth [12] for proving existence of three minimal patches in a given Euclidean tetrahedron, is based on the fact that a straight line on a minimal surface corresponds to a planar line of symmetry on the conjugate surface and vice versa. Minimal surfaces, which are cut by their symmetry planes in simply connected domains, have therefore a conjugate domain bounded by straight lines. To prove existence of the original piece one can often reconstruct the conjugate polygonal contour using only knowledge about the symmetry planes. Then e.g. the Morrey solution to the Plateau problem for the polygonal contour proves existence of the conjugate patch and via conjugation also of the patch bounded by symmetry planes which one was looking for. See Karcher [7] for conjugate constructions in $\mathbf{R}^3$, Karcher, Pinkall, Sterling [8] in $\mathbf{S}^3$ and Polthier [10] in $\mathbf{H}^3$.

3. Discrete minimal surfaces

In this paragraph we define discrete surfaces and analogs of other terms known from the continuous case. We will see that especially the energy of a discrete map and its derivative can be expressed in terms with geometric meaning.

Definition 2. *A* **discrete surface** *in a three dimensional space form is a topological simplicial complex consisting of triangles. The triangles may be degenerated to a line or a point.*

Definition 3. *A discrete surface is* **(area-) minimal** *iff small perturbations of surface vertices in a small region would increase the total area.*

In the following we assume that the discrete surfaces lie in a vector space attached with a constant metric. Let

$$f : (T_1, g) \to (T_2, h)$$

be a map between two triangulations with metrics g and h and with the same underlying topology, i.e. the abstract simplicial complexes of T_1 and T_2 are identical. We assume that f is defined on the vertices and continued as a linear map into the interior of the triangles. With this we define:

Definition 4. *The* **energy** *of a map between discrete surfaces is the sum of the energies of all linear triangular mappings*

$$f_i : (\Delta_{1,i}, g) \to (\Delta_{2,i}, h),$$

where $\Delta_{1,i}$ and $\Delta_{2,i}$ are the i-th corresponding triangles from T_1 and T_2 mapped onto each other by f_i.

The energies of these atomic maps f_i are given as in the continuous case. The f_i are linear mappings between two triangles, and their energy $E_D(f_i)$ is given by

$$\mathrm{E}_D(f_i) = \frac{1}{2} \int_{(\Delta_i, g)} |\nabla_g f_i|_h^2 ,$$

where ∇_g is the derivative operator w.r.t. the metric g and $|\cdot|_h$ the norm in image space w.r.t. the metric h.

It turns out that for a linear map $f : \Delta_1 \to \Delta_2$ between triangles Δ_1 and Δ_2 exists an explicit representation of $\mathrm{E}_D(f)$ in terms of the angles of Δ_1, i.e. its "conformal structure", and the side lengths of Δ_2:

Lemma 5. *Let f be a linear map between two triangles Δ_1 and Δ_2 in two vector spaces with constant metrics g and h. Then the Dirichlet energy of f is given by*

$$E_D(f) = \frac{1}{4}\sum_{i=1}^{3} \cot\alpha_i \cdot \left|\overrightarrow{a_i}\right|_h^2, \tag{2}$$

where α_i are the angles of Δ_1 w.r.t the metric g and a_i the corresponding side lengths in Δ_2 w.r.t. the metric h. See figure 1 for the notation.

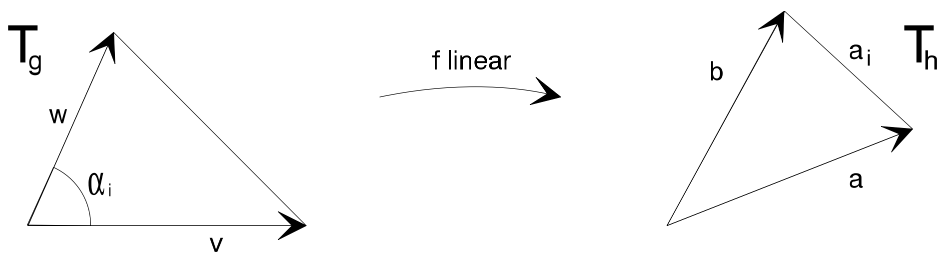

Figure 1: Atomic linear map between two triangles

Proof. The linear map is defined by $f(v) = a$ and $f(w) = b$ and its Dirichlet energy is given by

$$\mathrm{E}_D(f) = \frac{1}{2}\int_{T_g} |\nabla f|_h^2 = \frac{1}{2}\int_{T_g} tr\ h(\partial f., \partial f.)$$

We split f using two linear maps $\varphi : T_e \to T_g$ and $\psi : T_e \to T_h$. φ resp. ψ is given by mapping the unit base $\{e_1, e_2\}$ to $\{v, w\}$ resp. $\{a, b\}$ on the standard triangle T_e enclosed by the unit base $\{e_1, e_2\}$ in $\mathbf{R}^2$. Then we have $f = \psi \cdot \varphi^{-1}$ and $\partial f = \partial\psi \cdot \partial\varphi^{-1}$.

In the following the scalar products and norms are taken w.r.t the corresponding metric, we therefore skip indicating it.

It is:

$$^t\partial\psi \cdot \partial\psi = \begin{pmatrix} \langle a,a\rangle & \langle a,b\rangle \\ \langle a,b\rangle & \langle b,b\rangle \end{pmatrix}$$

$$\partial\varphi^{-1} \cdot^t \partial\varphi^{-1} = \begin{pmatrix} \langle w,w\rangle & -\langle v,w\rangle \\ -\langle v,w\rangle & \langle v,v\rangle \end{pmatrix} \cdot \tfrac{1}{(\det\partial\varphi)^2}$$

Therefore we compute:

$$\begin{aligned} tr(^t\partial f \cdot \partial f) &= tr(^t\partial\varphi^{-1} \cdot^t \partial\psi \cdot \partial\psi \cdot \partial\varphi^{-1}) \\ &= tr(^t\partial\psi \cdot \partial\psi \cdot \partial\varphi^{-1} \cdot^t \partial\varphi^{-1}) \\ &= \tfrac{1}{(\det\partial\varphi)^2} \cdot (\langle a,a\rangle \cdot \langle w,w\rangle - 2\langle a,b\rangle \cdot \langle v,w\rangle + \langle v,v\rangle \cdot \langle b,b\rangle) \end{aligned}$$

Defining $c := b - a$ we have $-2\langle a,b\rangle = |c|^2 - |a|^2 - |b|^2$ and continue with

$$\begin{aligned} &= \tfrac{1}{(\det\partial\varphi)^2} \cdot ((\langle w,w\rangle - \langle v,w\rangle)\,|a|^2 + (\langle v,v\rangle - \langle v,w\rangle)\,|b|^2 + \langle v,w\rangle\,|c|^2) \\ &= \tfrac{1}{\det\partial\varphi} \cdot (\tfrac{\langle -w,v-w\rangle}{\det\partial\varphi}\,|a|^2 + \tfrac{\langle w-v,-v\rangle}{\det\partial\varphi}\,|b|^2 + \tfrac{\langle v,w\rangle}{\det\partial\varphi}\,|c|^2) \\ &= \tfrac{1}{\det\partial\varphi} \cdot \textstyle\sum_{i=1}^{3} \cot\alpha_i\,|a_i|^2 \end{aligned}$$

For the last step we used the identities :

$$\cos\alpha = \frac{\langle v,w\rangle}{|v|\cdot|w|},\ \sin\alpha = \frac{\det\partial\varphi}{|v|\cdot|w|}.$$

Therefore we obtain:

$$\mathrm{E}_D(f) = \frac{1}{2}\int_{T_g} tr\ h(^t\partial f\partial f) = \frac{1}{2}\int_{Te} tr\ h(^t\partial f\partial f)\det\partial\varphi^{-1} = \frac{1}{4}\sum_{i=1}^{3}\cot\alpha_i\,|a_i|_h^2$$

(the additional factor $\frac{1}{2}$ is the area of T_e). $\square$

This representation is so natural that it should have appeared somewhere in the literature, but the authors have not found a reference. Compare Wilson [15] for a different and less clear examination of the triangular Dirichlet energy. Our representation immediately shows the conformal invariance of the Dirichlet energy w.r.t. conformal changes of the domain metric, and the quadratic dependence on the side lengths in image space.

As an immediate consequence we can now define the Dirichlet energy of a map f between two discrete surfaces as the sum of all energies on triangles:

$$\begin{aligned} \mathrm{E}_D(f) &= \textstyle\sum_{i=1}^{\#\ triangles} \mathrm{E}_D(f_i) \\ &= \tfrac{1}{4}\textstyle\sum_{i=1}^{\#\ edges}(\cot\alpha_i + \cot\beta_i)\,|a_i|^2 . \end{aligned} \tag{3}$$

In the last representation we merged two terms corresponding to the same edge a_i. The angles α_i and β_i are the angles opposite to a_i in the two adjacent triangles. For boundary edges one term is assumed to be zero. Heuristically the representation may be considered as the weighted sum of all edges lengths. The weights depend only on the domain. By this interpretation the energy is concentrated on the edges as tension. But be aware that the tension may be negative meaning that this edge acts with a repelling force on his end points.

We will proof some further useful identities for planar triangles.

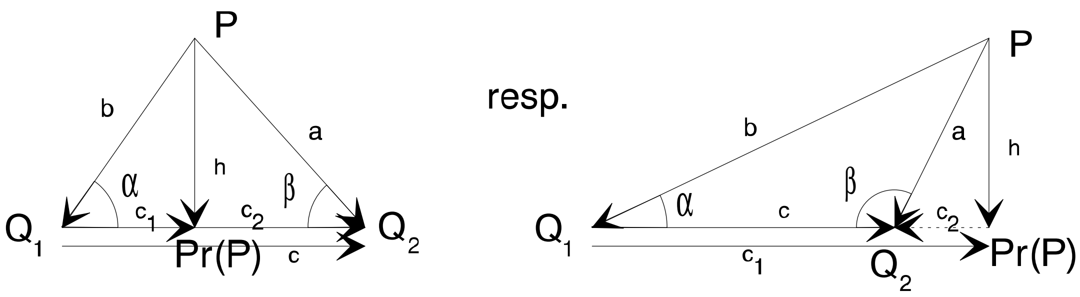

Figure 2: Notation for triangles

From figure 2 we read ($c_1 := \mathrm{Pr}(p) - q_1$, $c_2 := q_2 - \mathrm{Pr}(p)$, $c = c_1 + c_2 = q_2 - q_1$)

$$\begin{aligned} \cot\alpha \cdot h &= -D^{90} c_1 \\ \cot\beta \cdot h &= -D^{90} c_2 \\ a &= h + c_2 \\ b &= h - c_1 \end{aligned}$$

We now get immediately

$$\cot\alpha + \cot\beta = \tfrac{|c|}{|h|} \tag{4}$$

and further

$$\cot\alpha \cdot a + \cot\beta \cdot b = -D^{90} c \tag{5}$$

Computing formally the energy for the identity map of a triangle Δ with side lengths a, b, c and angles α, β, γ we obtain twice its area:

$$\cot\alpha \cdot |a|^2 + \cot\beta \cdot |b|^2 + \cot\gamma \cdot |c|^2 = 4 \cdot area(\Delta)$$

In the same way as in the continuous case we define a discrete harmonic map:

Definition 6. *A* **discrete harmonic map** *is a critical point for the Dirichlet energy functional w.r.t. variations of interior surface vertices in image space. To include symmetry properties into this definition we allow in some cases also variation of boundary points:*

- *if a domain boundary segment and its corresponding image boundary segment are straight lines, then the interior boundary points may vary along the straight line in image space*
- *if both corresponding segments are planar symmetry curves restricted to planes we allow variation of interior boundary points in the image plane. This models also free boundary value problems*
- *in all other cases the image boundary points remain fixed.*

The numerical condition for local harmonicity is explicitly given by differentiating expression (3):

$$\frac{\partial}{\partial p} E_D(f) = \frac{1}{2} \sum_{i=1}^{\#neighbours\ of\ p} (\cot \alpha_i + \cot \beta_i)(p - q_i) = 0 \tag{6}$$

$$\text{resp.} \quad p \quad = \quad \frac{\sum_{i=1}^{\#neighbours\ of\ p} (\cot \alpha_i + \cot \beta_i) q_i}{\sum_{i=1}^{\#neighbours\ of\ p} \cot \alpha_i + \cot \beta_i} \ ,$$

where q_i runs through all points adjacent to p. If (6) is true for all interior points p then f is a critical point for the discrete energy functional. The condition for points on boundary symmetry lines is the same except that the full vertex star around a point p has to be constructed corresponding to the symmetry properties.

We will now have a closer look at the procedure to compute the harmonic map numerically. For simplicity we assume a Dirichlet Problem, i.e. a given triangulated domain Ω and a fixed map $f : \partial\Omega \to \Gamma$, Γ a fixed polygonal contour, then looking for a harmonic extension of f into the interior of Ω. Solving problems with straight boundary lines or free boundary value problems the boundary points may also move but constraint to the current boundary condition.

Remark: 1. In the continuous case the extension is unique in Euclidean space. 2. In practice our algorithm uses $\partial\Omega = \Gamma$.

Let $P = (p_1, ..., p_B, p_{B+1}, ..., p_{B+I})$ be a representation of $f(\Omega)$ with $p_i, i > B$, an interior vertex of $f(\Omega)$ and $p_i, i \leq B$, a boundary vertex of $f(\Omega)$,. Then minimizing $E_D(f)$ is a quadratic problem and has a unique solution. We write it therefore using a quadratic form:

$$\begin{aligned} E_D(f) &= \tfrac{1}{4}\sum_{i=1}^{\#edges}(\cot\alpha_i + \cot\beta_i)\,|a_i|^2 \\ &= \tfrac{1}{8}\sum_{i=1}^{\#points}\sum_{j=1}^{\#neighbours\ of\ p_i}(\cot\alpha_{ij} + \cot\beta_{ij})\,|p_i - p_j|^2 \\ &= P^t \cdot S \cdot P \end{aligned}$$

where S is the well known stiffness matrix from finite element theory. But instead of having basis functions involved we have in our case explicit expressions for the components of S :

$$\begin{aligned} S_{ij} &= \begin{cases} -\frac{1}{8}(\cot\alpha_{ij} + \cot\beta_{ij})\cdot id & \text{, if } i \neq j \text{ and } p_i \text{ is adjacent to } p_j \\ 0 & \text{, if } i \neq j \text{ and } p_i \text{ is not adjacent to } p_j \end{cases} \\ S_{ii} &= \sum_{p_j = neighbour\ of\ p_i}(-S_{ij}) \end{aligned}$$

where id is the identity map of the ambient vector space. S is symmetric and positive definite ($0 \geq P^t \cdot S \cdot P \Leftrightarrow 0 \geq E_D(f) \geq area \Leftrightarrow P = 0$).

The condition for a surface to attain the minimum of the Dirichlet energy while keeping the boundary points fixed is given by: letting $X = (p_1, ..., p_B, x_{B+1}, ..., x_{B+I})$ be an admissible surface (with fixed boundary points p_i and free interior points x_i) and $\tilde{X} = (0, ..., 0, x_{B+1}, ..., x_{B+I})$ be an admissible variation direction we have

$$0 = \frac{\partial}{\partial \tilde{X}_{|X=P}} E_D(f) = \frac{\partial}{\partial \tilde{X}_{|X=P}} X^t \cdot S \cdot X = 2(0, ..., 0, id, ..., id) \cdot S \cdot X =: Q$$

$$\text{with } Q_i = \begin{cases} 0,\ i \in [1, B] \\ 2(\sum_{j=1}^{B} s_{ij}p_j + \sum_{j=B+1}^{B+I} s_{ij}x_j),\ i \in [B+1, B+I] \end{cases}.$$

The interior points x_i can be computed using the linear system of equations: $Q_i = 0,\ i \in [B+1, B+I]$.

Smooth harmonic maps defined on a planar domain are characterized by their mean value property, which means that the center of a small circle is mapped to the center of mass of the circle's image. This has as a consequence that the image of a harmonic map lies inside the convex hull of its boundary. For discrete harmonic maps a corresponding mean value property follows immediately from the local harmonicity condition (6), see Wilson [15]:

Lemma 7. *Let f be a discrete harmonic map defined on the points $\{q_i\}$ around a point p. If the points $\{q_i\}$ form a regular planar polyhedron with center p, then $f(p)$ is the center of mass of $\{f(q_i)\}$.*

But this result does not hold in general for other planar or spatial domains. Nevertheless we have a convex hull property for discrete harmonic maps as far as the spatial domain consists only of acute triangles.

Lemma 8. *Let f be a discrete harmonic map defined on a spatial domain formed by the points $\{q_i\}$ around a point p. If the triangles around p are all acute, then $f(p)$ lies in the convex hull of $\{f(q_i)\}$.*

Proof. From the local harmonicity condition (6) we see that p can be represented as a linear combination of the points $\{q_i\}$. Since all angles are acute, the weights of the q_i are in the interval $(0, 1.)$, and p is a convex combination.

Lemma 9. *Discrete minimal surfaces have the convex hull property, since they are critical points of the area functional.*

4. The Minimization Algorithm

In §3 we explained a method to compute a discrete harmonic map for an arbitrary given triangulated domain and a given boundary configuration Γ in image space. In that method Γ was allowed to consist of a collection of curves, which might individually be marked as being fixed curves or as being straight or planar symmetry lines. This would had the effect of additionally varying their boundary points w.r.t. these constraints. We call two collections Γ and Γ' equivalent ('$\sim$') iff both are identical along fixed arcs and if there exists a one to one correspondence of vertices inside a symmetry line resp. a symmetry plane.

Then our algorithm attacks the following problem:

Problem:. Given a boundary configuration Γ and an initial discrete surface M_0 with $\partial M_0 \sim \Gamma$. Find a discrete locally area minimizing surface M^* in the class

$$\begin{aligned} \mathbf{M} = \{M | M & \text{ two dimensional simplicial complex of the same} \\ & \text{combinatorial triangulation as } M_0 \text{ with } \partial M \sim \Gamma, \\ & M \text{ may be extended across symmetry arcs of } \partial M \text{ as a local minimizer}\} \end{aligned}$$

The problem is formulated in a very restrictive way as e.g. we do not allow topology changes for the moment. This constraint was made to simplify the description, see §6 for a discussion of topology changes.

The algorithm:

1. take the initial surface M_0 with boundary $\partial M_0 \sim \Gamma$ as the first approximation of M, set i to 0.

2. compute the next surface M_{i+1} by solving the linear Dirichlet problem

$$\min_M \frac{1}{2}\int_{M_i} |\nabla(f : M_i \to M)|^2 .$$

The condition for the minimum M_{i+1} is given by (6).

3. set i to $i+1$ and continue with 2.

Remark: In practice we use the criterium$|area(M_i) - area(M_{i+1})| < \epsilon$ as a stopping condition

Proposition 10. *The algorithm converges to a solution of the problem, if no triangles degenerate.*

Proof. The condition "no triangles degenerate" means that we assume all triangle angles for all surfaces of the sequence to be uniformly bounded away from 0 to π. From the construction the sequences $\{area(M_i)\}$ and$\{E_D(f_i : M_i \to M_{i+1})\}$ are monotone decreasing:

$$\begin{aligned} area(M_i) = E_D(id_{|M_i}) &\geq E_D(f_i : M_i \to M_{i+1}) \\ &= area(M_{i+1}) + E_C(f_i) \\ &\geq E_D(id_{|M_{i+1}}) = area(M_{i+1}) \end{aligned}$$

If no triangles degenerate we minimize in a compact set of surfaces. Therefore a subsequence of $\{M_i\}$ converges uniformly to a limit surface M, i.e. $|M_i - M| \to 0$. We now show that M is minimal: Let $\mathbf{M}$ be the above class of surfaces with the right topology and define

$$F_i : \mathbf{M} \to \mathbf{R}$$

$$F_i(X) := E_D(f_i : M_i \to X)$$

F_i is a quadratic function with minimum in M_{i+1}, i.e.

$$\nabla F_{i|M_{i+1}} = 0.$$

Because of the degeneracy condition we have a uniform bound $s_{\max}$ on the norm of $\nabla^2 F_i$ independent of i. Therefore

$$\nabla F_{i|M_i} = \nabla F_{i|M_i} - \nabla F_{i|M_{i+1}} = \nabla^2 F_{i|\xi} \cdot |M_i - M_{i+1}|^2$$

and we obtain:

$$\left|\nabla F_{i|M_i}\right| \leq s_{\max} \cdot |M_i - M_{i+1}|^2 .$$

Since we have $M_i \to M$ it follows $\nabla F_{i|M_i} \to \nabla F_{M|M} = 0$. $\nabla F_{M|M} = 0$ means that M is a critical point for the energy function $E_D(f_i : M \to X)$, i.e. M is stationary point for the area functional.□

5. The Conjugation Algorithm

One of the major problems conjugation algorithms have to deal with is that they have to use inaccurate discrete data out of a minimization process as an approximation to a smooth surface, since all known approaches try to simulate the procedure (1) of §2 for the smooth case.

The advantage of our method for discrete minimal surfaces, and far as the authors know, the only method with reasonable results, is that we use the discrete data of the minimization process directly to compute a discrete conjugate surface. The discrete minimality condition (6) is simultaneously the integrability condition for the discrete conjugate surface, which means that we loose no accuracy during the conjugation process.

The algorithm is defined for a triangular graph M, which is a stationary critical point for the area functional, but the algorithm may also be applied to harmonic maps between two discrete surfaces. Such a graph maybe obtained by a minimization procedure described in the previous paragraphs. Then for each vertex p we have the minimality condition

$$\frac{\partial}{\partial p} E_D(f : M \to X \in \mathbf{M})_{|X=M} = \frac{1}{2} \sum_{i=1}^{\#neighbours\ of\ p} (\cot \alpha_i + \cot \beta_i)(p - q_i) = 0,$$

which means geometrically that the sum of the weighted edges emanating from p add up to a closed polygon. This closed polygon is defined as the dual cell of the point p. This works perfectly for interior points. For points along the boundary we distinguish two case:

- If the point belongs to a planar or straight symmetry curve the whole neighbourhood is uniquely determined by the symmetry properties and the algorithm therefore works as for interior points.
- If a point p belongs to a non symmetric fixed boundary curve the construction of a neighbourhood is usually not possible. We then assume the existence of a neighbourhood such that all weighted edges sum up to zero. It is of no further relevance how this strip around the boundary curve is defined since for the conjugation algorithm it suffices to know only two adjacent boundary vertices of p and an edge from p into the interior of the surface.

So, how does the conjugation process work: consider a neighbourhood of a point p on the discrete minimal surface as in figure 3.

The identity map f of the discrete surface to itself is a discrete harmonic map by the assumption. Restricted to a single triangle it is a smooth linear map. Conjugation in the smooth case means rotating the one-form df of the map f in each tangent space.

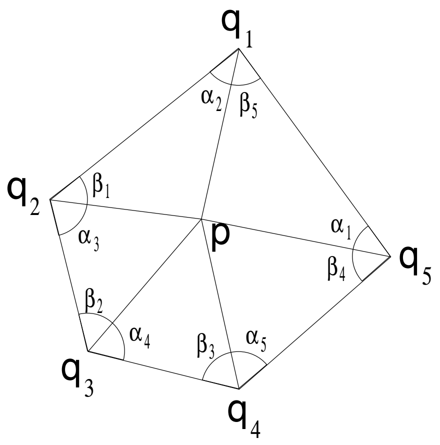

Figure 3: Neighbourhood around a Point

Here this operation is only defined on the smooth linear triangles, but along the edges it results in discontinuities of the atomic one-forms. In spite of these discontinuities the following definition makes sense:

We define a global star operator acting on the differential df of f by

$$*df := df \cdot J,$$

where J is the well-defined 90° rotation on the interior of each triangle.

The form $*df$ is not closed globally, but it turns out that it can be integrated along very special paths.

Consider two adjacent triangles in figure 4, which may not necessarily be coplanar.

Let v be the vector emanating from point p to point q, let further M_1, M_2 be the centers of the circumcircles of the triangles T_1, T_2 with w_1, w_2 being the mid perpendiculars w.r.t. the edge v. Then it is an elementary calculation that

$$\begin{aligned} w_1 &= \cot\alpha \cdot Jv \\ w_2 &= \cot\beta \cdot Jv \end{aligned}$$

where J is taken w.r.t. the appropriate triangle, and further

$$\begin{aligned} *df(w_1) &= -\cot\alpha \cdot v \\ *df(w_2) &= -\cot\beta \cdot v. \end{aligned}$$

This means $*df$ is continuous across triangle edges when applied to vectors orthogonally to the edges.

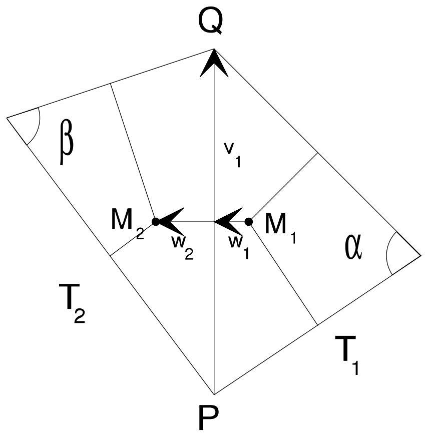

Figure 4: Path between two adjacent triangles

We now integrate the one-form $*df$ along the path γ, consisting of the mid perpendiculars around a point p. This results in adding up all the weighted vectors and we obtain

$$\int_\gamma *df = -\sum_{i=1}^{\#neighbours\ of\ p} (\cot\alpha_i + \cot\beta_i) v_i = 0.$$

Now we arrived at the most important point: The expression is exactly zero since it is the condition for the initial triangulation of being minimal, i.e.

Theorem 11. *The closeness condition for the dual one-form $*df$ equals the minimality condition for the initial triangulation f.*

$*df$ is therefore closed along such a path and in this way we obtain a dual cell for each vertex p. Continuing we get a well-defined dual graph to the given minimizing triangulation, see figure 5. For each triangle we obtain a vertex of the dual graph with three adjacent vertices. Every such four vertices lie in a plane since the three triangle edges were coplanar.

We are further interested in a triangulation of the dual surface being topologically equivalent to the original triangulation because then the associated family of the minimizing triangulation would also be defined. As remarked above this cannot be canonically defined since the one-form $*df$ is not globally closed. But we can continue integrating the form canonically on the interior of each triangle. This gives

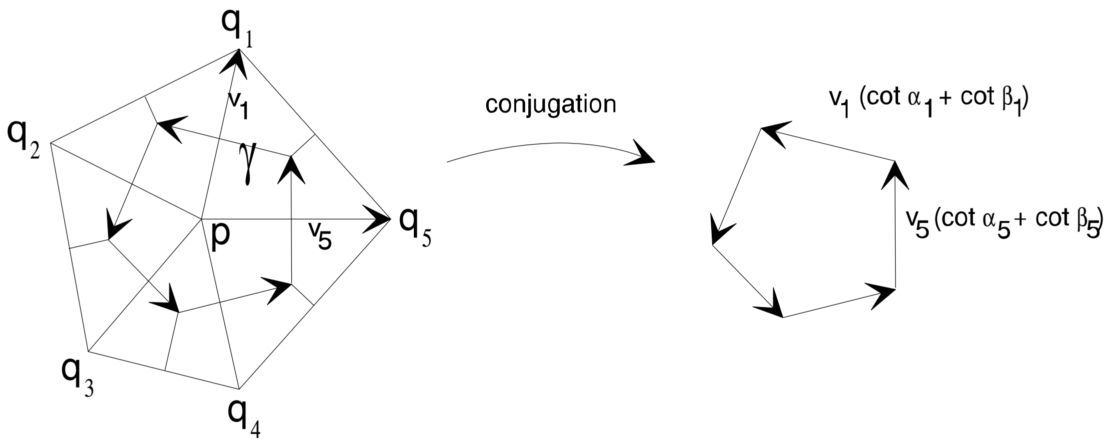

Figure 5: Integrating along a path: Integrating the atomic one form $*df$ along the path γ, consisting of all mid perpendiculars around a vertex p on the minimizing triangulation, gives the dual cell corresponding to p (for a clearer representation we d

a dual complex of triangles which fit together on common basis points of their mid-perpendiculars. A good approximation now for the center of each dual cell is taking the mean of all triangle vertices lying inside the dual cell, see figure 6.

In the case of a vertex q lying on a fixed boundary arc a whole neighbourhood is usually not contractible. To conjugate such points we use information available from the dual cell of an adjacent interior point. Look at figure 6 and assume q_i lies on a fixed boundary arc, p being an adjacent interior point. Then by conjugating a neighbourhood of p we automatically obtain $f_i^*(q_i)$ which is an ideal candidate for the dual point of q_i.Compared to the conjugation of interior points this method differs only in the fact that a final averaging is not possible.

Lemma 12. *In the case of a planar initial triangulation this results in getting exactly the conjugate minimal surface.*

Proof. In the planar case the operator J is constant on the triangulation, therefore $*df$ is globally closed on the triangulation T and being the differential of

$$f^* = -J \cdot f : T \to T^*,$$

mapping the triangulation T on its conjugate triangulation T^*, being the $90°$-rotated original triangulation T.

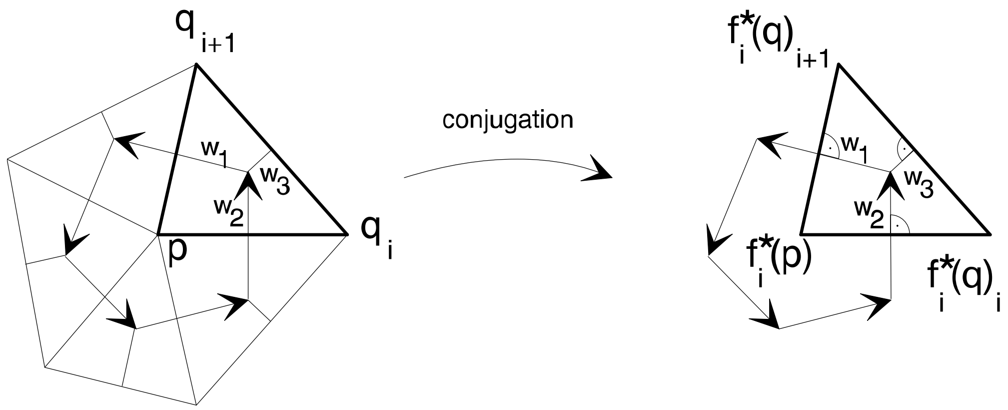

Figure 6: Conjugating a Cell: Integrating the atomic one form $*df$ inside the triangle (p, q_i, q_{i+1}) leads to a well-defined triangle, whose mid perpendiculars are part of the dual graph. The image $f^*(p)$ is defined as the mean of all $f_i^*(p)$.

A further property of the discrete conjugation method is given by the following lemma.

Lemma 13. *Straight lines resp. planar lines of symmetry of a minimizing triangulation are mapped to planar symmetry lines resp. straight lines on the conjugate triangulation.*

Proof. Let p be a boundary point lying on the interior of a straight line l with boundary neighbours q_1 and q_2. The vertex star around p consists of the boundary points q_1 and q_2, of points in the interior of the surface and their reflected images, see figure 7.

The dual cell is constructed by adding the weighted edges emanating from p in a circular sequence. Let v be a vector emanating from p. It can be written as

$$v = \ell + \ell^{\perp},$$

where $\ell^{\perp}$ denotes the component orthogonal to the line ℓ. The corresponding vector $rot(v)$ is given by

$$rot(v) = \ell - \ell^{\perp}.$$

We now start building the dual cell with the vector v_1^* parallel to ℓ, w.l.o.g putting the center of v_1^* into the origin. At its end point e we add the next vector v^* and at

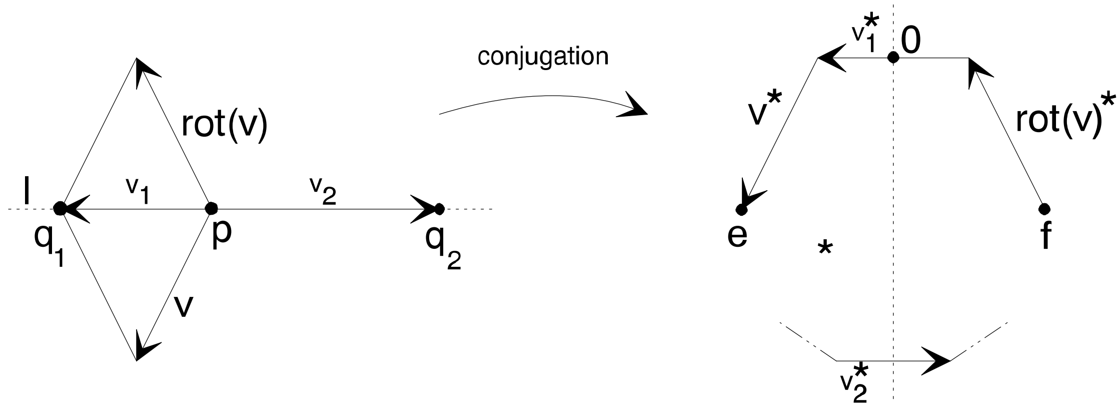

Figure 7: Symmetry of the Conjugate Surface

its foot point f the vector $-rot(v)^*$. The two new end points, also denoted with e and f, are given by

$$\begin{array}{rcl} e & = & \frac{1}{2}v_1^* + \ell + \ell^\perp \\ f & = & -\frac{1}{2}v_1^* - \ell + \ell^\perp \end{array} .$$

From this it follows by induction that the dual cell is symmetric w.r.t. the plane orthogonal to ℓ and going through the center of v_1^* and v_2^*.

In the same manner one proofs that planar symmetry lines are mapped to straight lines.□

6. Topology Changes

In this chapter we discuss ongoing experiments with changing the connectivity of a discrete surface during the minimization process. The aim of these experiments is to be able to compute beyond singular situations, when the triangulation becomes degenerate, and thereby compactifying the class of discrete surfaces occurring during the minimization process. "Degenerate triangulation" means that triangle angles become 0 or π. This happens when the triangle shrinks to a line, i.e all three points becoming collinear, or two or three vertices merge to a single point. From the theoretical point of view these situations are not dangerous since the energy and its derivative of a map of such a degenerate triangle to a non-degenerate would be infinite. Therefore the triangle would remain unchanged when continuing the iteration. The problems occur only for the numerics when triangles start to degenerate.

But it turns out that one can go around these difficulties by having a closer look at the degenerate situations. We consider the case where a vertex falls onto the opposite edge as a special case of the situation where two points merge.

Let A, B, C be a rectangular triangle as shown in figure 8,

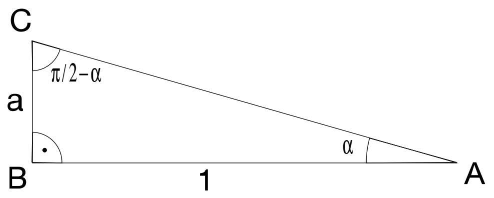

Figure 8: Degenerate Triangle

where the length $\overline{B,A}$ is normalized to unit length. Consider now the variation of the energy for variable C and small α:

The energy is given by

$$E = \frac{1}{4}(\cot\alpha\,|B-C|^2 + \cot(\frac{\pi}{2}-\alpha))$$

and

$$\begin{aligned} \tfrac{\partial}{\partial C}E &= \tfrac{1}{2}\cot\alpha(C-B) = \tfrac{1}{2}\cdot\tfrac{C-B}{|C-B|} \\ \tfrac{\partial^2}{\partial C^2}E &= \tfrac{1}{2}\cot\alpha\cdot id \end{aligned}$$

From this we have that moving C a little bit while α is very small would cost an infinite amount of energy. So once having a degenerate triangle it will remain degenerate during further minimizations. The consequence for the numerical algorithm is that we can compute beyond singular situations: once such a situation occurs we can simply remove the singular triangle using the rules shown in figure 9.

The total number of triangles is less or equal than before.

References

[1] K. Brakke, *Surface Evolver Manual*, The Geometry Center, Minneapolis.

[2] P. Concus, *Numerical Solution of the Minimal Surface Equation*, Math. Comput. 21 (1967), 340-350.

[3] R. Courant, *Dirichlet's Principle, Conformal Mapping, and Minimal Surfaces*, Interscience, New York, 1950.

[4] J. Douglas, *Solution of the Problem of Plateau*, Trans. Amer. Math. Soc. **33** (1931), 263-321.

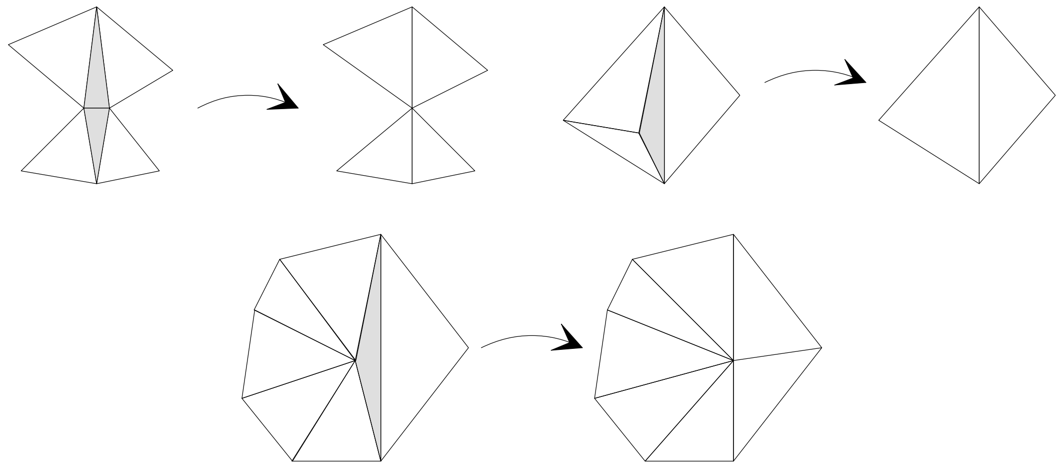

Figure 9: Degenerate Situations

[5] G. Dziuk, *An Algorithm for Evolutionary Surfaces*, Numer. Math. 58 (1991), 603-611.

[6] J.E. Hutchinson, *Computing Conformal Maps and Minimal Surfaces*, Proc. Centr. Math. Anal., Canberra, **26** (1991), 140-161.

[7] H. Karcher, *Triply Periodic Minimal Surfaces of Alan Schoen and Their Constant Mean Curvature Companions*, Manuscr. Math. 64 (1989), 291-357.

[8] H. Karcher, U. Pinkall, I. Sterling, *New Minimal Surfaces in S^3*, J. Diff. Geom. 28 (1988), 169-185.

[9] H.B. Lawson, *Complete Minimal Surfaces in S^3*, Ann. of Math. **92** (1970), 335-374.

[10] K. Polthier, *New Periodic Minimal Surfaces in H^3*, Proc. Centr. Math. Anal., Canberra, **26** (1991), 201-210.

[11] T. Rado, *The Problem of Least Area and the Problem of Plateau*, Math. Z. 32 (1930), 763-796.

[12] B. Smyth, *Stationary Minimal Surfaces with Boundary on a Simplex*, Invent. Math. **76** (1984), 411-420.

[13] J.M. Sullivan, *A Crystalline Approximation Theorem for Hypersurfaces*, Ph.D. thesis, Princeton Univ. (1990).

[14] T. Tsuchiya, *Discrete Solutions of the Plateau Problem and Its Convergence*, Math. of. Comp. **49**, 179 (1987),157-165.

[15] W.L. Wilson, *On Discrete Dirichlet and Plateau Problems*, Num. Math. **3** (1961), 359-373.

[16] O. Wohlrab, *Zur numerischen Behandlung von parametrischen Minimalflächen mit halbfreien Rändern*, Dissertation Bonn, 1985.

7.
Figures

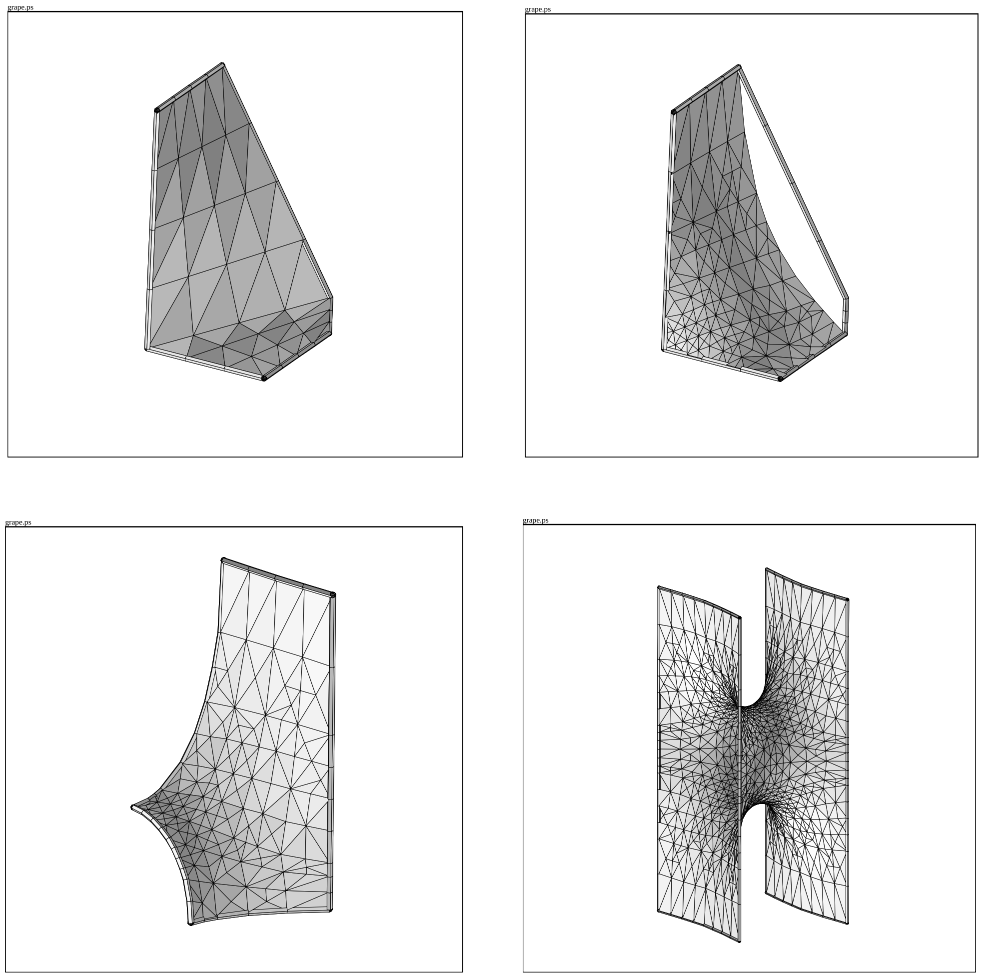

Figure 10: Constructing Karcher's Scherk surface with handle

Initial triangulation of a pentagon in fig. 10a with four straight and one planar boundary. Boundary points may vary along straight arcs resp. planes. Figure 10b shows the triangulation after some minimization steps. Applying the conjugation algorithm leads to fig. 10c with four exactly planar and one exactly straight symmetry line. Successive reflection along symmetry lines leads to a fundamental domain for the translation group of the complete minimal surface of Karcher. Refining was controlled by using discrete curvature information of the discrete surface.

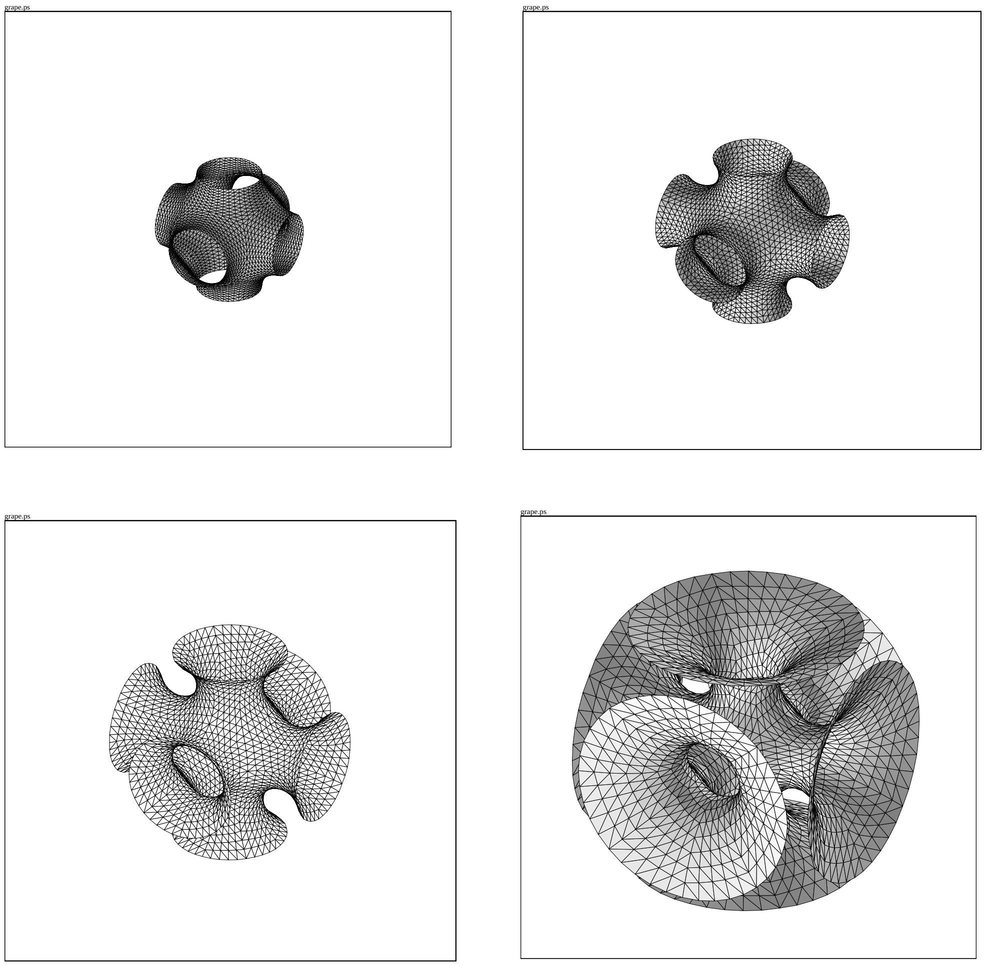

Figure 11: Minimal surface with ends

The initial surfaces of the sequence are bounded by three straight lines meeting at angles 60° and 90°, and a helicoidal arc having 90° angles with two straight lines. The helicoidal arc is translated to infinity during the sequence. The conjugate piece consists of three planar symmetry lines and and eighth of a catenoidal end. It can be reflected to a minimal surface with cubical symmetry and six growing ends, which approximates a complete minimal surface in the limit. The helicoidal arc in this example is no symmetry line.

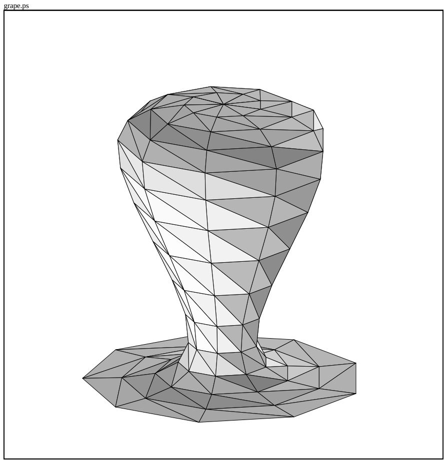

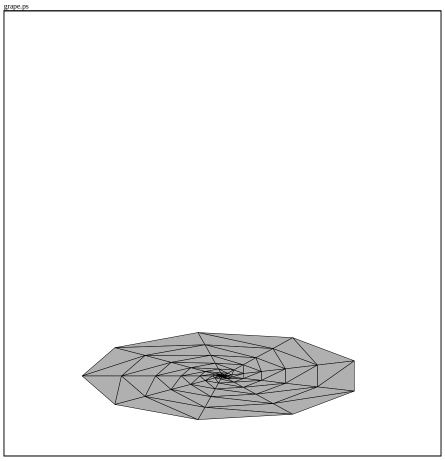

Figure 12: Minimizing a drop-like surface

A drop-like initial surface bounded by a planar curve. One minimization step leads directly to a planar surface, and therefore avoids a mean curvature flow type singularity at the thin neck. This illustrates that the minimization algorithm proceeds discrete also in time direction.

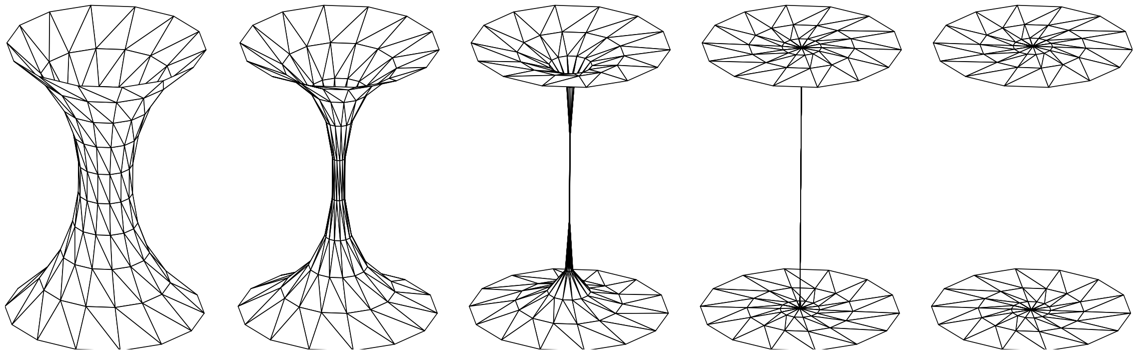

Figure 13: The Goldschmidt solution

All minimization steps of a cylinder type initial surface. Between the Goldschmidt solution and the final figure an additional algorithm removing degenerate triangles was applied.

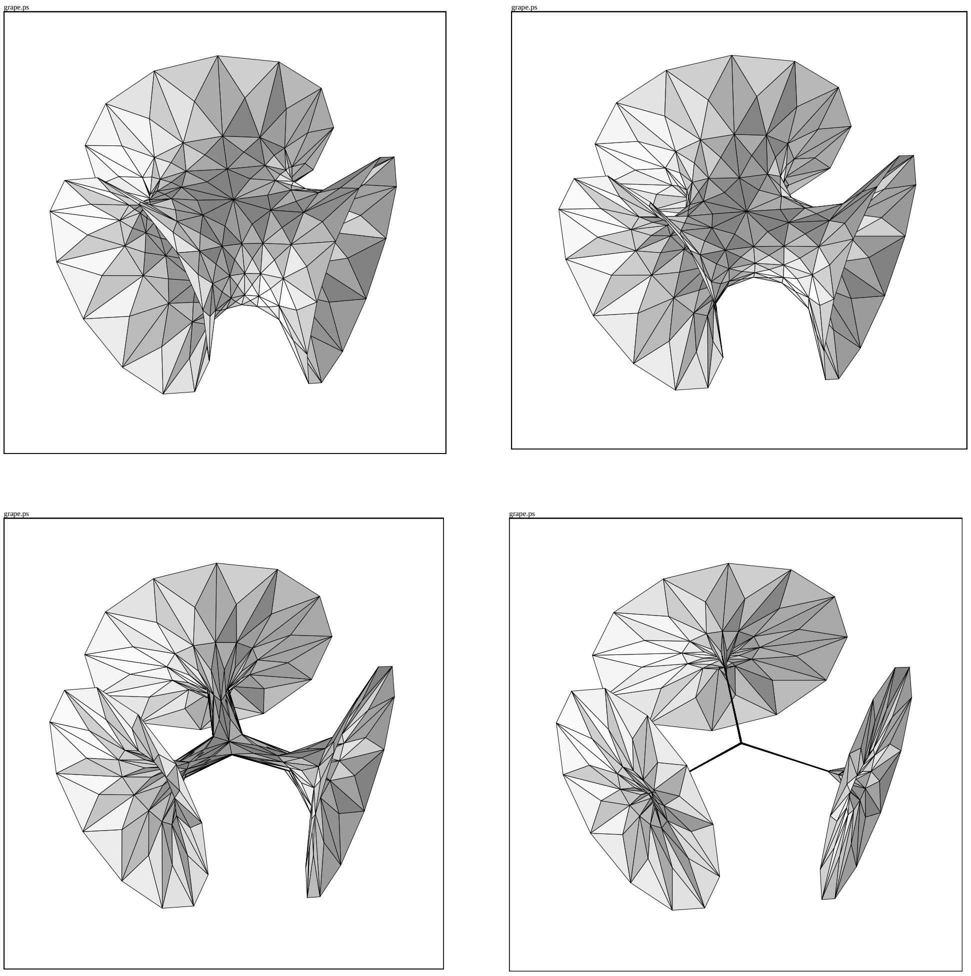

Figure 14: Minimizing the instable Trinoid

An example similar to fig. ?? with higher genus. An instable part of the trinoid minimal surface of Jorge and Meeks was computed using the Weierstraß representation formula and then used as an initial surface for the minimization algorithm. The same Goldschmidt type solution as in fig. ?? appears.

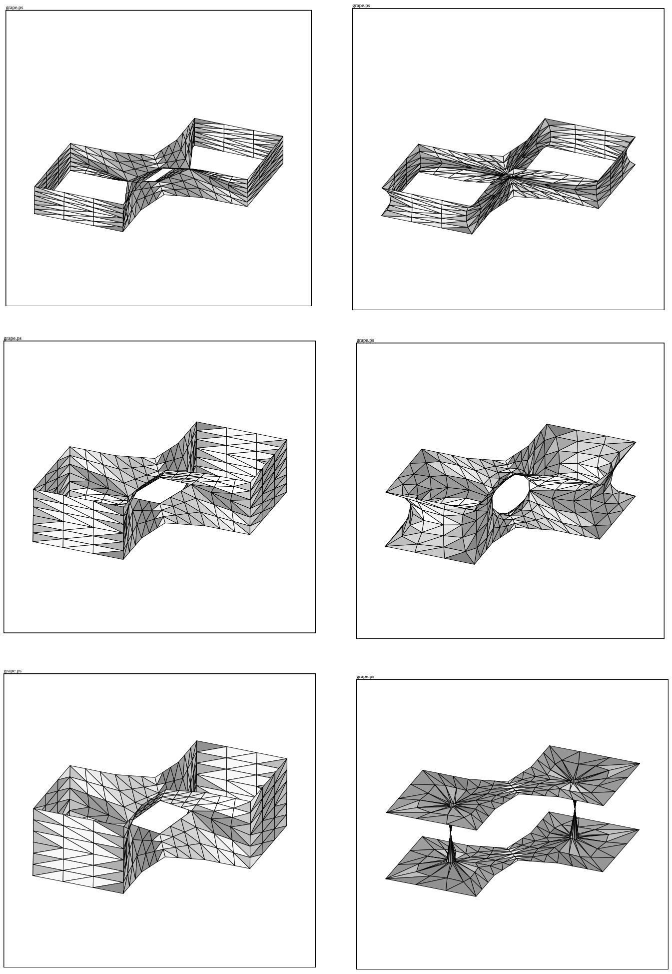

Figure 15: Surface with higher genus

A one-parameter family of initial surfaces where the distance between both figure-eight boundary curves is varying. Depending on the height three situations appear during the minimization procedure. Two extreme height values lead to two different singularities, once a singularity at the middle neck and once two singularities at the two outer necks. For special height values a stable discrete minimal surfaces is obtained in the limit. The initial surfaces were generated using the surface builder module of GRAPE.

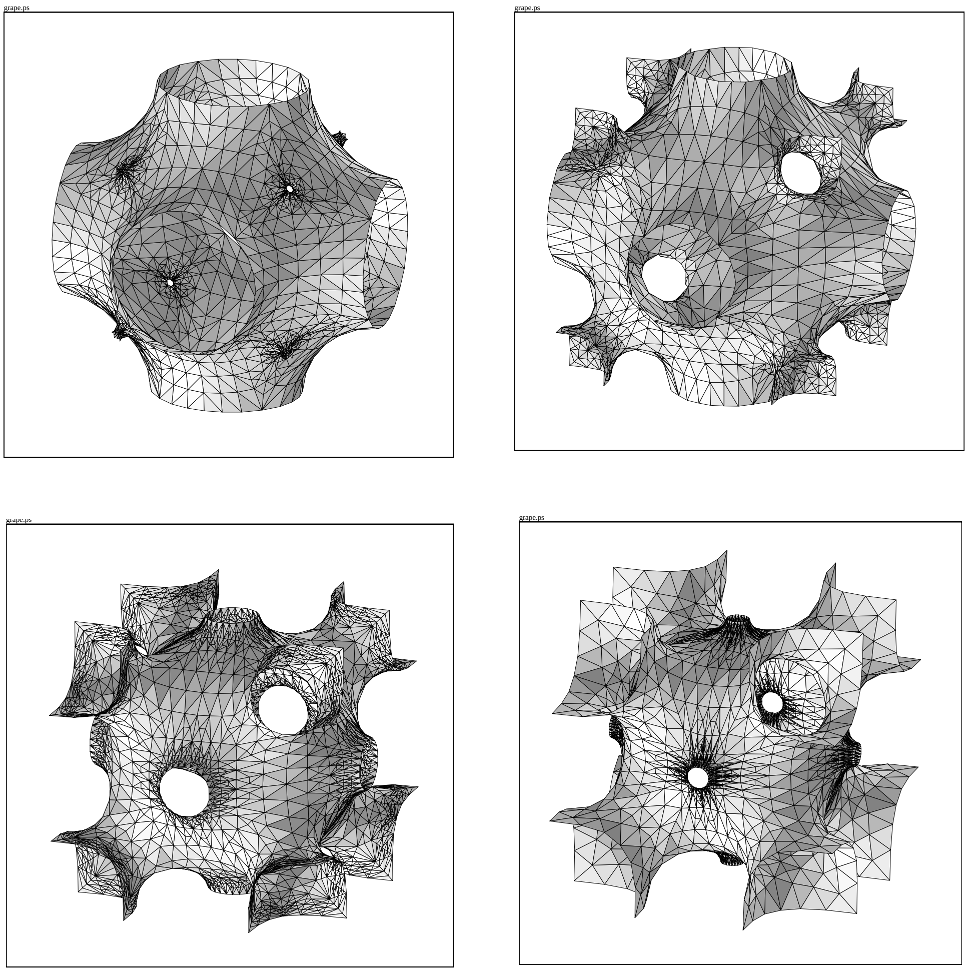

Figure 16: Growing Karcher handles

This example illustrates the time dependent process of growing additional handles out of existing minimal surfaces. For the O,C-TO surface of A. Schoen is no representation formula known, its existence was proved by Karcher [7] as an intermediate value argument using the conjugate surface construction, i.e. during the process of growing handles exists one value at which the handles meet the existing symmetry planes of the cube. The occurring extreme situations made it necessary to refine adaptively during the deformation. Refining was controlled by using discrete curvature information of the discrete surface.

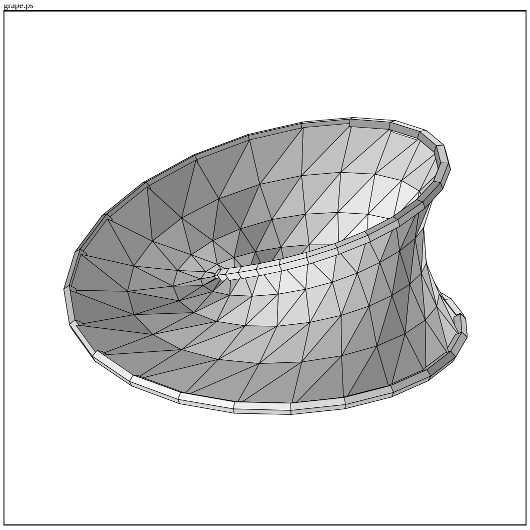

Figure 17: A non orientable minimal Möbius band

The algorithm handles non orientable surfaces since the dirichlet minimality condition (6) is independent of the orientation.

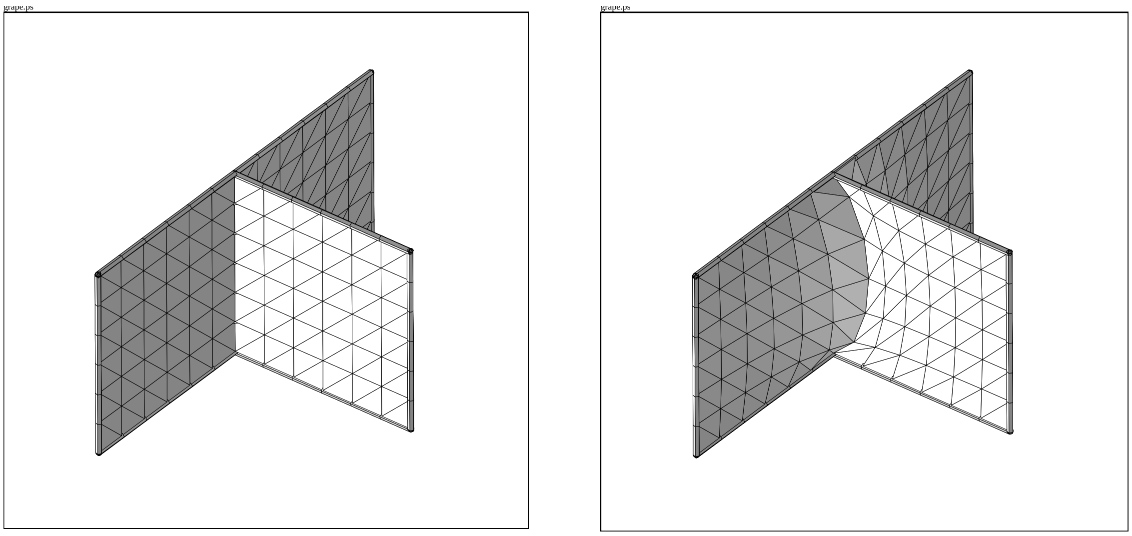

Figure 18: A Surface with triple line

A minimal configuration with a singular triple line where three patches meet. Such multiple lines are naturally covered by the algorithm since the dirichlet minimality condition at a point (6) is a finite sum of the weighted directions of all edges emenating from a point. The weight of each edge is determined by all triangles, which may be more than two, joining this edge.

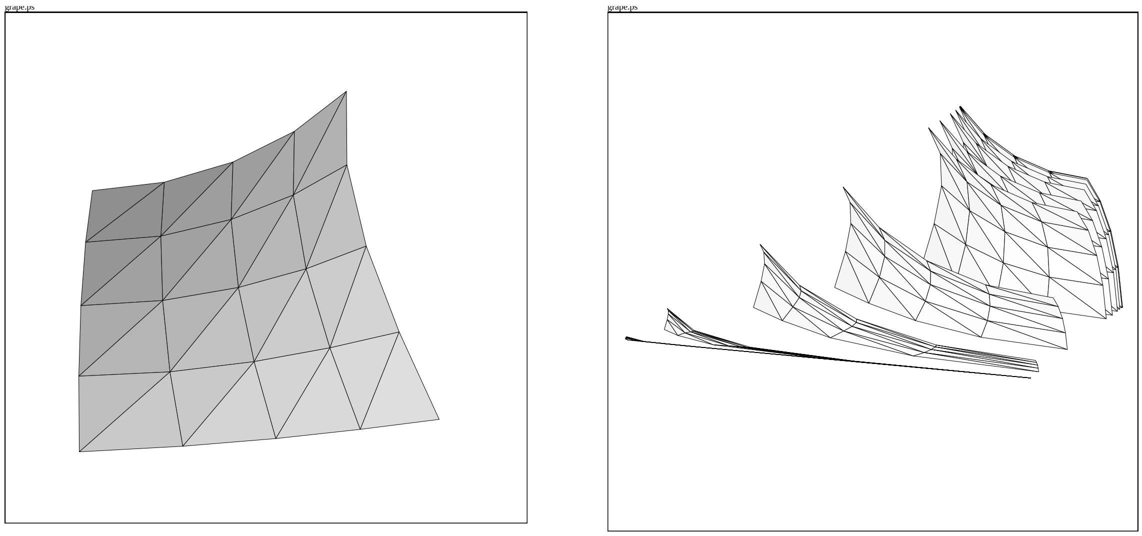

Figure 19: Examples of Smyth in a tetrahedron

An example corresponding to the first usage of the conjugate surface construction by B. Smyth. A discrete minimal surface in a quadrilateral is conjugated to a patch bounded by the four faces of a tetrahedron along planar symmetry lines. But this patch is not a stable discrete minimal surface. Further minimization of this patch while keeping the boundary curves restricted to the faces lets the patch degenerate to an edge of the tetrahedron.

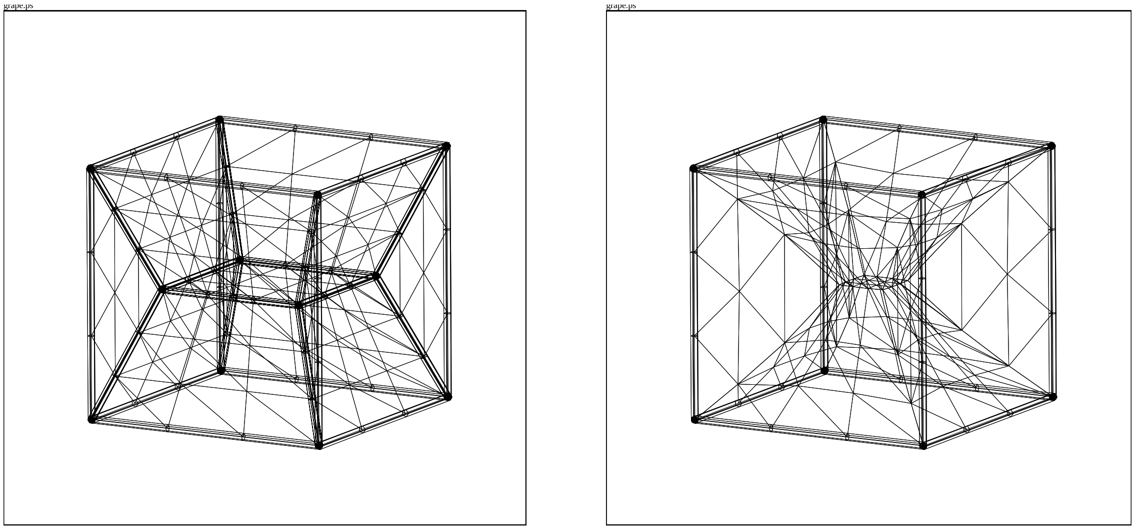

Figure 20: Minimal Surface Configuration in a Cube

A minimal configuration bounded by the edges of a cube. The interior of the surface contains triple lines where different surface patches meet at an angle of $120°$.